Spherical voids in the stabilized jellium model: Rigorous theorems and Padé representation of the void-formation energy

Paul Ziesche*
Helsinki University of Technology, Laboratory of Physics, 02150 Espoo, Finland

John P. Perdew
Department of Physics and Quantum Theory Group, Tulane University, New Orleans, Louisiana 70118

Carlos Fiolhais
Department of Physics, University of Coimbra, 3000 Coimbra, Portugal
(Received 20 September 1993)

We consider the energy needed to form a spherical hole or void in a simple metal, modeled as ordinary jellium or stabilized jellium. (Only the latter model correctly predicts positive formation energies for voids in high-density metals.) First we present two Hellmann-Feynman theorems for the void-formation energy $4\pi R^2\sigma_R^v(\bar{n})$ as a function of the void radius R and the positive-background density $\bar{n}$, which may be used to check the self-consistency of numerical calculations. They are special cases of more-general relationships for partially emptied or partially stabilized voids. The difference between these two theorems has an analog for spherical clusters. Next we link the small-R expansion of the void surface energy (from perturbation theory) with the large-R expansion (from the liquid drop model) by means of a Padé approximant without adjustable parameters. For a range of sizes (including the monovacancy and its "antiparticle," the atom), we compare void formation energies and cohesive energies calculated by the liquid drop expansion (sum of volume, surface, and curvature energy terms), by the Padé form, and by self-consistent Kohn-Sham calculations within the local-density approximation, against experimental values. Thus we confirm that the domain of validity of the liquid drop model extends down almost to the atomic scale of sizes. From the Padé formula, we estimate the next term of the liquid drop expansion beyond the curvature energy term. The Padé form suggests a "generalized liquid drop model," which we use to estimate the edge and step-formation energies on an Al (111) surface.

I. INTRODUCTION

Vacancies determine many properties of metals, which are interesting from a technological point of view. Inside irradiated metals, they form vacancy clusters or voids often filled with pressurized He gas (bubbles). For sufficiently high implantation doses, voids form regular arrays (void lattices).

Vacancies and voids are characterized by static and thermodynamic properties like electron density, formation energy, enthalpy, and entropy,[1–8] and by dynamic properties like energy-loss spectra and (curved) surface plasmons. The lifetime of positrons provides an experimental tool to study voids.[9]

We focus on the void formation energy (at zero temperature). Such energies and other properties have been calculated within the jellium model, an idealized model in which the positive charge of the ions is smeared out into a uniform positive background.[2,10–17] The results and failures of the jellium model and pseudopotential perturbation theory have been summarized in Ref. 14. Full *ab initio* treatments for vacancies in Na and Al have been done; see Refs. 18–20 and references therein. Vacancies (and self-interstitials) in bcc Li are studied in Ref. 21, where a short survey is given of calculations for atomic defects in metals. Therein different influences on the theoretical value of the vacancy formation energy are critically reviewed: the local-density approximation (LDA) and the underestimated lattice constant following from it, the effective potential and the need for full-potential calculations, the structural relaxation around the vacancy, the size convergence of supercell calculations, and Brillouin-zone sampling. *Ab initio* calculations for 3*d* and 4*d* transition metals were done in Refs. 8, 22, and 23. Those calculations were based on the Korringa-Kohn-Rostoker–Green's-function (KKR-GF) method.[24] Divacancies (in Cu, Ni, Ag, and Pd) and nearly spherical voids[25] (in Cu) were also treated by this method.

While voids have negatively curved surfaces, clusters have positively curved surfaces. Total energy calculations for clusters depending on size (number of atoms) and structure are the counterparts to calculations of void formation energies. A review of such cluster calculations within the jellium model is given in Ref. 26. Results of void and cluster calculations have sometimes been compared with each other.[27,28]

Other examples of particularly curved solid surfaces are quarter-space solids (or wedges) with rounded or unrounded edges.[29,30] Terraces or single straight ledges or steps, of interest for the understanding of crystal growth,[31] have been considered recently, as have regularly stepped (vicinal) surfaces[32] and wavy steps.

The jellium model often serves as an important reference system modeling *sp*-bonded or simple metals, al-

though it has intrinsic deficiencies (e.g., the planar surface energy and the void formation energy for the valence electron density of Al are negative[2,33]). These deficiencies are rectified by pseudopotential corrections,[33–35] which may be treated perturbatively,[33–35] variationally,[17,36] or exactly. Recently, a structureless pseudopotential model or stabilized jellium model has been proposed.[37,39] Its idea is similar to those of Ashcroft and Langreth,[35] Brovman, Kagan, and Holas[40,41] (where calculations without the second- and higher-order terms correspond to stabilized jellium), Heine and Hodges,[42] and Monnier and Perdew.[36] It has the simplicity and universality of the jellium model, but avoids some of its deficiencies. Bulk properties,[37] planar surface properties,[37,39,43–46] and curved surface properties[28,38,44] have been investigated in the framework of stabilized jellium. Sophisticated calculations of Pb surface properties have been compared with a similarly modified jellium model.[47] Planar surface properties of stabilized jellium have been studied in terms of correlated many-body wave functions.[48] The "structure-averaged jellium model" of Ref. 49 is (essentially) the stabilized jellium model slightly modified, and applied to clusters with a self-adjusting background.[50] The plasmon resonance in Li clusters has been studied with a "pseudo-jellium model."[51]

In this paper, we study the energetics of spherical voids of arbitrary size in an otherwise-homogeneous stabilized jellium. First we present two rigorous theorems for the void surface energy as a function of the void radius R and of the stabilized jellium density $\bar{n}$. They are consequences of the Hellmann-Feynman theorem

$$\partial E_\lambda/\partial\lambda=\langle\Psi_\lambda|\partial\hat{H}_\lambda/\partial\lambda|\Psi_\lambda\rangle ,$$

where $\hat{H}_\lambda\Psi_\lambda=E_\lambda\Psi_\lambda$. The derivatives with respect to R and $\bar{n}$ are related to the electric field arising from the dipole layer at the background edge, to the number of electrons that have spilled out into the vacuum region, and to the electron density at the background edge. Such theorems serve to check numerical calculations. To derive the void theorems, we need first to derive a (Hellmann-Feynman) theorem for stabilized jellium spheres, which generalizes a formerly derived and numerically checked theorem for ordinary jellium spheres.[52,53] We show how our void theorems (whose nonstabilized versions have been derived in Refs. 52 and 54) are related to a theorem which has been derived for voids in ordinary jellium by Finnis and Nieminen.[15] And we study the limiting case of large void radius $R\to\infty$. Theorems recently derived and illustrated for the planar surface emerge in this limit.[46] They modify theorems provided by Budd and Vannimenus[55–58] for ordinary jellium.

In addition to these sum-rule studies, we link the small-R expansion of the void surface energy

$$\sigma_R^v=aR+bR^3+cR^4+O(R^5) \tag{1}$$

with the large-R expansion

$$\sigma_R^v=\sigma-\frac{\gamma}{2R}+O\left[\frac{1}{R^2}\right] \tag{2}$$

by means of a Padé approximant. [From the perturbation theory, it follows that there is no term $\sim R^2$ in Eq. (1), and that, for stabilized jellium, a vanishes.] The small-R coefficients, resulting from perturbation theory either directly or via the void theorems, contain the bulk energy of ordinary jellium, for which we use the expression of Ref. 59, and the dielectric function from linear response theory (with an appropriate local field correction[60]). The large-R coefficients are obtained from self-consistent planar surface calculations[44] of σ and γ, the latter found with the help of the fourth-order gradient expansion for the kinetic energy. σ and γ are the surface tension and the curvature energy, natural parameters of the liquid drop model.[44,61–63] This model proposes for weakly curved surfaces a curved-surface energy of $\sigma A+\frac{1}{2}\gamma\int dA\,\mathcal{R}^{-1}$, where $\mathcal{R}^{-1}$ is the local curvature (negative for a concave surface). With the help of the Padé form, this model may be generalized[30] to strongly curved surfaces down to the Wigner-Seitz radius r_0. The Padé form of σ_R^v with the substitution $R\to -R$ describes the nonoscillatory part of the cluster surface energy σ_R^c. The surface energy of a single atom, $\sigma_{r_0}^c$ (or $\sigma_{-r_0}^v$) determines the cohesive energy $4\pi r_0^2\sigma_{r_0}^c$. Liquid drop and Padé results for monovacancy formation energies are compared here with self-consistently calculated values[28] and with experimental data. Finally, we apply the generalized liquid drop model to edges and steps, and compare the step formation energy so estimated for a step on an Al(111) surface with the value recently obtained from sophisticated calculations.[31]

Our present work is a detailed explanation and extension of a brief preliminary report.[30]

II. THE SYSTEM, ITS CHARACTERISTIC QUANTITIES, AND RIGOROUS THEOREMS

We consider a spherical void with radius R in an otherwise-homogeneous (stabilized or ordinary) jellium with valence electron density $\bar{n}=3/4\pi r_s^3$. (Atomic units, bohr$=\hbar^2/me^2$ and hartree$=me^4/\hbar^2$, are used throughout.) The positive-background density profile $\bar{n}\theta(r-R)$, where θ is the Heaviside step function, is neutralized by the corresponding electron density, $n_R^v(r)$. Here $R=N^{1/3}z^{1/3}r_s$, where z is the valence and N is the number of removed atoms. Mathematically, R and $\bar{n}$ are independent variables, i.e., $(4\pi/3)R^3\bar{n}$ need not be an integer. The case $N=1$ or $R=r_0$, with $r_0=z^{1/3}r_s$ being the Wigner-Seitz radius, corresponds to a monovacancy. The number of electrons that have spilled into the void region $r<R$ (divided by the void surface area) is

$$\nu_R^v=\int_0^R dr\left[\frac{r}{R}\right]^2 n_R^v(r) .$$

The dipole layer near the void surface causes an electric field $\mathcal{E}_R^v(\mathbf{r})=\mathcal{E}_R^v(r)\mathbf{r}/r$ [with $\mathcal{E}_R^v(r)<0$], and, via $\mathcal{E}_R^v(r)=d\phi_R^v(r)/dr$ and $\phi_R^v(\infty)=0$, a corresponding potential $\phi_R^v(r)$ which goes smoothly from positive values inside the void to zero for distances far away from it.

The void formation energy is the energy to form the void by digging out the positive background from the void region $r<R$ at the center of a large neutral sphere

(with radius R_1), adding it at the outer surface (up to a radius $R_2 > R_1$) and finally taking the limit $R_1 \to \infty$ of an infinitely large reference sphere. [Note that for any given background density $\bar{n}$, the expression $(4\pi/3)R_1^3\bar{n} = N_1$ must be an integer.] So the background density profile of the reference system, $n_+(r) = \bar{n}\theta(R_1 - r)$, is changed by adding the void perturbation[64]

$$n_+^v(r) = -\bar{n}\theta(R - r) + \bar{n}\theta(r - R_1)\theta(R_2 - r) , \tag{3}$$

with R_2 fixed by $\int d^3r\, n_+^v(r) = 0$; hence $R_2^3 - R_1^3 = R^3$. The corresponding ground-state energies E (of the large reference sphere) and E_R (of the enlarged sphere with the void inside) define for $R_1 \to \infty$ the void formation energy

$$4\pi R^2 \sigma_R^v = (E_R - E)|_{R_1 \to \infty} . \tag{4}$$

σ_R^v, the void formation energy per unit area, we call the void surface energy. The formation energy of a monovacancy is $4\pi r_0^2 \sigma_{r_0}^v$.

The many-body Hamiltonian for the reference sphere is

$$\hat{H} = \hat{T} + \int d^3r \left\{ \frac{1}{2}\frac{1}{4\pi} P[\hat{\mathcal{E}}(\mathbf{r})]^2 - n_+(r)\left[\bar{e} + \frac{de}{d\bar{n}}\hat{n}(\mathbf{r}) \right] \right\} . \tag{5}$$

Here the second square-bracket term in the potential energy operator is the stabilization correction. The electric-field operator $\hat{\mathcal{E}}(\mathbf{r})$ arises from the charge density $n_+(r) - \hat{n}(\mathbf{r})$, where

$$\hat{n}(\mathbf{r}) = \sum_i^{N_1} \delta(\mathbf{r} - \mathbf{r}_i)$$

is the electron-density operator. P deletes the divergent self-interaction, so

$$P\hat{n}(\mathbf{r})\hat{n}(\mathbf{r}') = \sum_i \sum_{j \neq i} \delta(\mathbf{r} - \mathbf{r}_i)\delta(\mathbf{r}' - \mathbf{r}_j)$$

is the pair distribution function operator. Finally, $\bar{e} = \frac{3}{5}(z^{2/3}/r_s)$ and e = bulk energy (per electron) of ordinary jellium. (For the details of the stabilization correction, see Ref. 37.) The ground-state energy of $\hat{H}$ is E, needed in Eq. (4).

E_R is the ground-state energy of the void Hamiltonian $\hat{H}_R$ arising from the reference Hamiltonian $\hat{H}$ by adding to its background density $n_+(r) = \bar{n}\theta(R_1 - r)$ the void perturbation (3). So we have $\hat{H}_R = \hat{H} + \hat{H}_R^v$ with

$$\hat{H}_R^v = \int d^3r \left[\frac{1}{4\pi}\hat{\mathcal{E}}(\mathbf{r})\cdot\mathcal{E}_+^v(\mathbf{r}) + \frac{1}{2}\frac{1}{4\pi}[\mathcal{E}_+^v(\mathbf{r})]^2 - \frac{de}{d\bar{n}} n_+^v(r)\hat{n}(\mathbf{r}) \right] , \tag{6}$$

where $\mathcal{E}_+^v(\mathbf{r})$ is the electric field due to $n_+^v(r)$. The last term of Eq. (6) arises from the stabilization correction.

From the many-body Hamiltonians for the void problem, the following sum rules can be derived straightforwardly using the Hellmann-Feynman theorem:

$$[\bar{n} - n(0)]\frac{de}{d\bar{n}} = \int_{-\infty}^0 ds\, \mathcal{E}(s) , \tag{7}$$

$$3\bar{n}\frac{\partial}{\partial\bar{n}}\sigma_R^v = \frac{\bar{n}}{R^2}\int_R^\infty dr(r^3 - R^3)\mathcal{E}_R^v(r) + 3\left[\left[\bar{n}\frac{d}{d\bar{n}} \right]^2 e \right] \nu_R^v , \tag{8}$$

$$\left[R\frac{\partial}{\partial R} + 2 \right]\sigma_R^v = \bar{n}R\left[\int_R^\infty dr(-1)\mathcal{E}_R^v(r) - \int_{-\infty}^0 ds\, \mathcal{E}(s) \right] + \bar{n}\frac{de}{d\bar{n}} R[n_R^v(R) - n(0)] , \tag{9}$$

where $\mathcal{E}(s)$ is the electric field of a semi-infinite stabilized jellium (occupying the half-space $s < 0$) and $n(0)$ is the electron density at its a planar (flat) surface. As an example of how to proceed, the void theorem (8) is proved in Appendix A. Other Hellmann-Feynman theorems for partially emptied or partially stabilized voids are presented in Appendixes B and C, respectively.

Of course, the right-hand sides (rhs's) of Eqs. (7)–(9) can be written equivalently (but see remark added to Ref. 55) in terms of the potentials $\phi_R^v(r)$ and $\phi(s)$, instead of the electric fields $\mathcal{E}_R^v(r)$ and $\mathcal{E}(s)$. And to each of Eqs. (7)–(9) there corresponds a theorem for ordinary jellium: In Eq. (7), $n(0)$ must be deleted; in Eqs. (8) and (9), the last terms must be deleted. Note that $n_R^v(r)$, hence also $\mathcal{E}_r^v(r)$ and σ_R^v, change if the stabilization correction is switched off. The theorem (7) follows from Eq. (F14) of Ref. 36, with $C = -\bar{n}de/d\bar{n}$ and $X = 0$. It is the stabilized version of the Budd-Vannimenus theorem.[55]

The nonstabilized versions of Eqs. (8) and (9) with $\phi_R^v(r)$ on the rhs have been derived in Refs. 52 and 54. Their difference agrees—if use is made of the nonstabilized version of Eq. (7)—with a theorem given by Finnis and Nieminen[15] and rederived in Ref. 65. The analogous difference of Eqs. (8) and (9) yields the relation

$$\left[3\bar{n}\frac{\partial}{\partial\bar{n}} - R\frac{\partial}{\partial R} - 2 \right]\sigma_R^v = -\bar{n}R\left[\int_R^\infty dr \left[\frac{r}{R} \right]^3 (-1)\mathcal{E}_R^v(r) - \int_{-\infty}^0 ds\, \mathcal{E}(s) \right] + 3\left[\left[\bar{n}\frac{d}{d\bar{n}} \right]^2 e \right] \nu_R^v - \bar{n}\frac{de}{d\bar{n}} R[n_R^v(R) - n(0)] , \tag{10}$$

which compares with a corresponding theorem for neutral spherical clusters, modeled by stabilized jellium spheres:

$$\left[3\bar{n}\frac{\partial}{\partial\bar{n}} - R\frac{\partial}{\partial R} - 2 \right]\sigma_R^c = \bar{n}R\left[\int_0^R dr \left[\frac{r}{R} \right]^3 \mathcal{E}_R^c(r) - \int_{-\infty}^0 ds\, \mathcal{E}(s) \right] + 3\left[\left[\bar{n}\frac{d}{d\bar{n}} \right]^2 e \right] \nu_R^c + \bar{n}\frac{de}{d\bar{n}} R[n_R^c(R) - n(0)] . \tag{11}$$

Here the cluster surface energy (per unit area) σ_R^c follows from the total energy of the stabilized jellium sphere via

$$E_R^c=\frac{4\pi}{3}R^3\bar{n}(e+\Delta e)+4\pi R^2\sigma_R^c \ .$$

Here $\Delta e=-\bar{e}-\bar{n}\,de/d\bar{n}$ is the stabilization correction of the bulk energy; for a "cluster" consisting of only one atom, i.e., $(4\pi/3)R^3\bar{n}=z$ or $R=r_0$, the quantity $4\pi r_0^2\sigma_{r_0}^c$ is the cohesive energy.[61] $\nu_R^c=\int_R^\infty dr(r/R)^2 n_R^c(r)$ represents the number of electrons (per unit area) that have spilled out into the vacuum region. Equation (11) follows from Eq. (A4), if R_1 and E are replaced respectively by R and E_R^c and use is made of Eq. (7). The original expression on the left-hand side of Eq. (11) is $(3\bar{n}\partial/\partial\bar{n}-2)\sigma_R^c$, with the constraint $N=$const. Equation (11) emerges under the assumption that an interpolation between integer values of N makes σ_R^c a continuous smooth function of $\bar{n}$ *and* R.

The reason why the sphere theorem (11) does not split into two separate theorems analogous to the void theorems (8) and (9) is as follows: For a void, the quantities $\bar{n}$ and R are independent (real positive) variables, whereas for a neutral sphere they vary subject to the constraint $\bar{n}4\pi R^3/3=$positive integer.

The nonstabilized version of the theorem (11), i.e., without the last two terms on the rhs, was derived in Ref. 52 and numerically checked by Ekardt *et al.*[53]

Finally, with $R\to\infty$ the limiting cases of infinitely large voids and spheres are recovered. With the planar (flat) surface energy σ of stabilized jellium and with $\nu=\int_0^\infty ds\, n(s)$, we have

$$\sigma_R^v\to\sigma,\quad \nu_R^v\to\nu,\quad -\mathcal{E}_R^v(R-s)\to\mathcal{E}(s)\ ,$$

$$\sigma_R^c\to\sigma,\quad \nu_R^c\to\nu,\quad \mathcal{E}_R^c(R+s)\to\mathcal{E}(s)\ ,$$

and from Eqs. (8), (9), and (11) we obtain

$$\frac{d\sigma}{d\bar{n}}=\int_{-\infty}^0 ds\, s\mathcal{E}(s)+\left[\frac{d}{d\bar{n}}\left[\bar{n}\frac{de}{d\bar{n}}\right]\right]\nu\ , \tag{12}$$

$$2\sigma=+\bar{n}R[\phi_R^v(R)-\phi(0)]|_{R\to\infty}+\bar{n}\frac{de}{d\bar{n}}R[n_R^v(R)-n(0)]|_{R\to\infty}\ , \tag{13}$$

$$2\sigma=-\bar{n}R[\phi_R^c(R)-\phi(0)]|_{R\to\infty}-\bar{n}\frac{de}{d\bar{n}}R[n_R^c(R)-n(0)]|_{R\to\infty}\ . \tag{14}$$

With $\phi_R^v(\infty)=\phi_R^c(0)=\phi(-\infty)=0$, the potentials are gauged to zero deep in the bulk for each case.

The nonstabilized version of Eq. (12), i.e., without the last term on the rhs, is just the Vannimenus-Budd theorem[58] for the surface energy of ordinary jellium. The nonstabilized version of Eq. (14) has been derived in Ref. 66. For a numerical illustration of the theorems (7) and (12), see Ref. 46. They are the first of a hierarchy of force sum rules leading from the bulk via surfaces and edges to corners, as shown in Refs. 29, 66, and 67 for ordinary jellium.

With the expansion

$$\phi_R^v(R)=\phi(0)+\phi_1^v\frac{1}{R}+\frac{1}{2!}\phi_2^v\frac{1}{R^2}+O\left[\frac{1}{R^3}\right]$$

and an analogous one for $n_R^v(R)$, Eq. (13) takes the form

$$\sigma=\frac{1}{2}\left[\bar{n}\phi_1^v+\bar{n}\frac{de}{d\bar{n}}n_1^v\right]\ , \tag{15}$$

and, with Eqs. (2) and (15), from Eq. (9) we obtain

$$\gamma=\bar{n}\phi_2^v+\bar{n}\frac{de}{d\bar{n}}n_2^v\ . \tag{16}$$

With the expansion

$$-\mathcal{E}_R^v(R-s)=\mathcal{E}(s)+\mathcal{E}_1^v(s)\frac{1}{R}+O\left[\frac{1}{R^2}\right]$$

from Eqs. (8) and (12), we obtain

$$\frac{d\gamma}{d\bar{n}}=2\int_{-\infty}^0 ds[-s^2\mathcal{E}(s)+s\mathcal{E}_1^v(s)]+2\left[\frac{d}{d\bar{n}}\left[\bar{n}\frac{de}{d\bar{n}}\right]\right]\nu_1^v\ . \tag{17}$$

In nuclear theory, expansions in powers of R^{-1} are referred to as leptodermous expansions.[44,61,62] For relations like Eqs. (15) and (16) obtained from the ordinary jellium model for metal clusters, see Ref. 68.

III. PERTURBATION TREATMENT OF SMALL VOIDS

A simple "physical" derivation of the small-R expansion for the energy of a spherical void in ordinary jellium is presented in Appendix D. In this section, we focus on stabilized jellium.

For small voids, $\hat{H}_R^v$ from Eq. (6) can be treated as a perturbation. The eigenvalues and eigenstates of the unperturbed reference Hamiltonian $\hat{H}$ from Eq. (7) are E_n and $|n\rangle$, respectively (with E and $|0\rangle$ for the ground state).

The lowest-order contribution to σ_R^v arises from $4\pi R^2\sigma_R^{v(1)}=\langle 0|\hat{H}_R^v|0\rangle|_{R_1\to\infty}$ with

$$\langle 0|\hat{H}_R^v|0\rangle=\int d^3r\left[\frac{1}{4\pi}\mathcal{E}(r)\mathcal{E}_+^v(r)+\frac{1}{2}\frac{1}{4\pi}[\mathcal{E}_+^v(r)]^2-\frac{de}{d\bar{n}}n_+^v(r)n(r)\right]\ , \tag{18}$$

where $\mathcal{E}(r)$ and $n(r)$ refer to the unperturbed reference sphere. It is easy to show that

$$\sigma_R^{v(1)}=-\frac{\bar{n}}{3}\int_{-\infty}^0 ds\ \mathcal{E}(s)R+\frac{4\pi}{15}\bar{n}^2R^3-\frac{\bar{n}}{3}\frac{de}{d\bar{n}}[-\bar{n}+n(0)]R\ . \tag{19}$$

Due to theorem (7), the first and the last terms of Eq. (19) cancel each other. So, for stabilized jellium, there is no contribution $\sim R$. For ordinary jellium, the last term is not present and the void surface energy is $\sim R$ for small R. The second term is just the electrostatic self-energy of

$n^{v}_{+}(r)$, which does not influence any many-body property of the homogeneous jellium.

The next-order contribution to σ^{v}_{R} arises from

$$4\pi R^2\sigma^{v(2)}_R=-\sum_{n\neq 0}\frac{\langle 0|\hat{H}^{v}_{R}|n\rangle\langle n|\hat{H}^{v}_{R}|0\rangle}{E_n-E}\bigg|_{R_1\to\infty}. \quad (20)$$

Because of $\langle n|0\rangle=\delta_{n,0}$, only the following terms of $\hat{H}^{v}_{R}$ contribute to Eq. (20):

$$\Delta\hat{H}^{v}_{R}=\int d^3r\left[\frac{1}{4\pi}\hat{\mathcal{E}}_{-}(\mathbf{r})\cdot\mathcal{E}^{v}_{+}(\mathbf{r})-\frac{de}{d\bar{n}}n^{v}_{+}(r)\hat{n}(\mathbf{r})\right],$$

where $\hat{\mathcal{E}}_{-}(\mathbf{r})$ arises only from the electron charge density operator $-\hat{n}(\mathbf{r})$. A trivial rewriting of $\Delta\hat{H}^{v}_{R}$ is

$$\Delta\hat{H}^{v}_{R}=\int d^3r\left[\phi^{v}_{+}(r)-\frac{de}{d\bar{n}}n^{v}_{+}(r)\right]\hat{n}(\mathbf{r}),$$

or, in reciprocal space [with the Poisson equation $-q^2\tilde{\phi}^{v}_{+}(q)=4\pi\tilde{n}^{v}_{+}(q)$],

$$\Delta\hat{H}^{v}_{R}=\int\frac{d^3q}{(2\pi)^3}\left[-\frac{4\pi}{q^2}-\frac{de}{d\bar{n}}\right]\tilde{n}^{v}_{+}(q)\hat{n}(\mathbf{q}). \quad (21)$$

$\tilde{n}^{v}_{+}(q=0)=0$ expresses the neutrality of the void perturbation (3). With the linear response expression

$$-\sum_{n\neq 0}\frac{\langle 0|\hat{n}(\mathbf{q})|n\rangle\langle n|\hat{n}(\mathbf{q}')|0\rangle}{E_n-E}\to\frac{1}{2}(2\pi)^3\delta(\mathbf{q}+\mathbf{q}')\frac{\chi(q)}{\bar{\epsilon}(q)},$$

and with the Fourier transform of $n^{v}_{+}(r)$

$$\tilde{n}^{v}_{+}(q)\to-\bar{n}\tilde{\theta}(qR)$$

[both expressions are valid in the limit $R_1\to\infty$, and

$$\tilde{\theta}(qR)=\frac{4\pi}{3}R^3\frac{3j_1(qR)}{qR}$$

where

$$j_1(x)=\frac{\sin x-x\cos x}{x^2}$$

is the transform of $\theta(R-r)$], we obtain

$$4\pi R^2\sigma^{v(2)}_R=\frac{1}{2}\int\frac{d^3q}{(2\pi)^3}\left[\frac{4\pi}{q^2}+\frac{de}{d\bar{n}}\right]^2\times[-\bar{n}\tilde{\theta}(qR)]^2\frac{\chi(q)}{\bar{\epsilon}(q)}. \quad (22)$$

$\chi(q)$ is the Lindhard function

$$\chi(q)=-\frac{3}{2}\frac{\bar{n}}{e_F}l\left(\frac{q}{2k_F}\right),\qquad l(x)=\frac{1}{2}\left[1+\frac{1}{2x}(1-x^2)\ln\left|\frac{1+x}{1-x}\right|\right], \quad (23)$$

where $k_F=(3\pi^2\bar{n})^{1/3}$, $e_F=k_F^2/2$, and

$$\bar{\epsilon}(q)=1-\frac{4\pi}{q^2}\chi(q)[1-G(q)] \quad (24)$$

contains the local field correction $G(q)$ beyond the random phase approximation.[69] Within LDA,[70] we have

$$G(q)=-\frac{1}{4\pi}\frac{d^2}{d\bar{n}^2}(\bar{n}e_{xc})\,q^2, \quad (25)$$

according to Ref. 60. We take the bulk exchange-correlation energy per electron e_{xc} from Ref. 59.

A more explicit rewriting of Eq. (22) is

$$\sigma^{v(2)}_R=\frac{4}{9}\bar{n}^2\int_0^\infty dq\left[\frac{3j_1(qR)}{qR}\right]^2\times\left[\frac{4\pi}{q^2}+2\frac{de}{d\bar{n}}+\left[\frac{de}{d\bar{n}}\right]^2\frac{q^2}{4\pi}\right]\frac{\chi(q)}{\bar{\epsilon}(q)}R^4. \quad (26)$$

To extract from Eq. (26) the coefficients of the small-R expansion (1), we make use of the asymptotic behavior of the spherical Bessel function j_1 for $x\to 0$, where the term $\sim(de/d\bar{n})^2$ needs special treatment due to the asymptotic behavior of the integrand for large q. With $q^2\chi(q)/\bar{\epsilon}(q)\to-4\bar{n}$ following from Eq. (23), we can rewrite Eq. (26) as

$$\sigma^{v(2)}_R=-\frac{4}{9\pi}\bar{n}^3\left[\frac{de}{d\bar{n}}\right]^2\int_0^\infty d(qR)\left[\frac{3j_1(qR)}{qR}\right]^2R^3+\frac{4}{9}\bar{n}^2\int_0^\infty dq\left[\frac{3j_1(qR)}{qR}\right]^2\left[\left[\frac{4\pi}{q^2}+2\frac{de}{d\bar{n}}\right]\frac{\chi(q)}{\bar{\epsilon}(q)}+\left[\frac{de}{d\bar{n}}\right]^2\frac{1}{4\pi}\left[4\bar{n}+\frac{q^2\chi(q)}{\bar{\epsilon}(q)}\right]\right]R^4. \quad (27)$$

Now, in the first term,

$$\int_0^\infty dx\,[3j_1(x)/x]^2=3\pi/5$$

applies (so we obtain an additional term $\sim R^3$), whereas in the second term $3j_1(x)/x\to 1$ for $x\to 0$ leads to the term $\sim R^4$. As shown in Appendixes B and C, the small-R expansion of $\sigma^{v}_R=\sigma^{v(1)}_R+\sigma^{v(2)}_R$ according to Eqs. (19) and (26) can be confirmed by rigorous theorems and coupling-constant integrations mentioned in Sec. II.

In summary, the coefficients of the small-R expansion (1) are $a=0$ [respectively, $-(\bar{n}^2/3)(de/d\bar{n})$ for ordinary jellium], and

$$b=\frac{4}{15}\bar{n}^2\left[\pi-\bar{n}\left[\frac{de}{d\bar{n}}\right]^2\right], \quad (28)$$

$$c=\frac{4}{9}\bar{n}^2\int_0^\infty dq\left[\left[\frac{4\pi}{q^2}+2\frac{de}{d\bar{n}}\right]\frac{\chi(q)}{\tilde{\epsilon}(q)}+\left[\frac{de}{d\bar{n}}\right]^2\frac{1}{4\pi}\left[4\bar{n}+\frac{q^2\chi(q)}{\tilde{\epsilon}(q)}\right]\right]. \quad (29)$$

All stabilization corrections vanish at the equilibrium bulk density of jellium ($de/d\bar{n}=0$ at $r_s=4.19$).

In linear response, the next term in the power expansion of $j_1(x)$ in Eq. (27) gives rise to terms of higher order than R^4. And from higher-order perturbation theory (quadratic response), we expect no further contribution to the R^4 term, since the perturbation is of order R^3 and its second-order or R^6 contribution to $4\pi R^2\sigma_R^v$ formally requires only the linear response of the density.

IV. PADÉ APPROXIMATION AND NUMERICAL RESULTS

The small-R limit of Eq. (1) and the large-R limit of Eq. (2) are linked by a simple Padé approximant

$$\sigma_R^v=\sigma\frac{1+A_1(Nz)^{-1/3}+A_2(Nz)^{-2/3}}{1+B_1(Nz)^{-1/3}+B_2(Nz)^{-2/3}+B_3(Nz)^{-1}}. \quad (30)$$

For a metal with density parameter r_s, the void radius $R=(Nz)^{1/3}r_s$ is determined by z (the valence) and N (the number of removed atoms). The coefficients for the Padé approximation are obtained from the coefficients of the limits (1) and (2) by simple algebra:

$$B_3=\frac{\sigma-\frac{(ar_s)}{\sigma}\left[\frac{\gamma}{2r_s}\right]+\frac{(ar_s)^3}{\sigma(br_s^3)}}{(br_s^3)-\frac{(ar_s)^2(cr_s^4)}{\sigma(br_s^3)}}\rightarrow\frac{\sigma}{(br_s^3)}, \quad (31)$$

$$B_2=-\frac{(ar_s)+(cr_s^4)B_3}{(br_s^3)}\rightarrow-\frac{\sigma(cr_s^4)}{(br_s^3)^2}, \quad (32)$$

$$B_1=\frac{\sigma-(br_s^3)B_3}{(ar_s)}\rightarrow\frac{(\gamma/2r_s)}{\sigma}, \quad (33)$$

$$A_2=\frac{(ar_s)}{\sigma}B_3\rightarrow 0, \quad (34)$$

$$A_1=\frac{(ar_s)}{\sigma}B_2\rightarrow 0, \quad (35)$$

The arrows indicate the limiting case $a\rightarrow 0$, which holds for stabilized jellium (and for ordinary jellium at its equilibrium density, i.e., $r_s=4.19$).

The results for the small-R coefficients a,b,c, according to Eqs. (28) and (29) and the remark before Eq. (28), are presented in Table I. The results for the large-R coefficients σ (planar surface energy) and γ (curvature energy) according to Ref. 44 are presented in Table II. Table II also contains, for the densities of Al, Na, and Cs, the results obtained from self-consistent local-density calculations of voids in stabilized jellium[28] with the Perdew-Wang[59] electron-gas input (as used in all tables and figures of this paper). These results suggest a "rule" $\gamma/\sigma\approx 2$ or 3 bohr. Recent full-potential KKR-GF calculations for unrelaxed nearly spherical voids in fcc Cu (lattice constant $=6.76$ bohr),[25] together with self-consistent half-space and bulk calculations, suggest[71] that $\sigma=37.1$ meV/bohr^2 and $\gamma=58.9$ meV/bohr.

Table III gives the Padé coefficients A_1, A_2, B_1, B_2, and B_3 for voids in stabilized (and in ordinary) jellium at the densities of Al, Mg, Na, and Cs. From these, we can estimate the coefficient of the next term of the liquid drop expansion (2) beyond $\gamma/2R$, describing curvature in higher order (interaction between different parts of the curved surface):

$$4\pi R^2\sigma_R^v=4\pi R^2\sigma-2\pi R\gamma+\delta+\cdots. \quad (36)$$

This extended liquid drop expansion, compared with the Padé approximation of Eq. (30), yields

$$\delta=4\pi r_s^2\sigma(A_2-A_1B_1+B_1^2-B_2)\rightarrow 4\pi r_s^2\sigma(B_1^2-B_2). \quad (37)$$

TABLE I. Coefficients a, b, and c of the small-R expansion (1), according to Eqs. (28) and (29) and the remark before Eq. (28), for ordinary jellium (J) and stabilized jellium (SJ): (in millihartree/bohr^2; r_s in bohr). (1 millihartree/bohr^2=27.21 meV/bohr^2=1557 erg/cm^2.)

		ar_s		br_s^3		cr_s^4	
Metal	(r_s)	J	SJ	J	SJ	J	SJ
H	(1.58)	−6.100	0	12.105	9.774	−15.121	−30.114
Al	(2.07)	−1.698	0	5.383	4.851	−7.525	−12.848
Zn	(2.30)	−0.998	0	3.924	3.644	−5.733	−9.170
Pb	(2.30)	−0.998	0	3.924	3.644	−5.733	−9.170
Mg	(2.65)	−0.464	0	2.566	2.459	−3.979	−5.794
Li	(3.24)	−0.129	0	1.404	1.385	−2.372	−2.977
Ca	(3.27)	−0.121	0	1.366	1.349	−2.316	−2.886
Sr	(3.57)	−0.057	0	1.049	1.044	−1.849	−2.142
Ba	(3.71)	−0.038	0	0.935	0.932	−1.675	−1.877
Na	(3.93)	−0.016	0	0.787	0.786	−1.446	−1.536
K	(4.86)	0.019	0	0.416	0.414	−0.841	−0.715
Rb	(5.20)	0.022	0	0.340	0.336	−0.709	−0.554
Cs	(5.62)	0.022	0	0.269	0.264	−0.582	−0.410

TABLE II. Coefficients of the large-R expansion (2): Planar surface energy σ and curvature energy γ, according to the planar-surface calculations of Ref. 44, for ordinary jellium (J) and stabilized jellium (SJ): (r_s in bohr; σ and $\gamma/2r_s$ in millihartree/bohr^2). Results in parentheses are from fits to the results of self-consistent void calculations (Ref. 28).

		σ		$\gamma/2r_s$	
Metal	(r_s)	J	SJ	J	SJ
H	(1.58)	−3.320	0.759	0.890	1.049
Al	(2.07)	−0.390	0.595	0.442	0.442
			(0.594)		(0.395)
Zn	(2.30)	−0.067	0.479	0.318	0.309
Pb	(2.30)	−0.067	0.479	0.318	0.309
Mg	(2.65)	0.108	0.342	0.197	0.189
Li	(3.24)	0.142	0.200	0.098	0.094
Ca	(3.27)	0.141	0.195	0.094	0.091
Sr	(3.57)	0.128	0.152	0.068	0.066
Ba	(3.71)	0.121	0.136	0.059	0.057
Na	(3.93)	0.109	0.115	0.047	0.046
			(0.115)		(0.045)
K	(4.86)	0.067	0.061	0.020	0.021
Rb	(5.20)	0.056	0.049	0.016	0.016
Cs	(5.62)	0.045	0.038	0.016	0.012
			(0.039)		(0.013)

As in Eqs. (31)–(35), the arrow refers to stabilized jellium (or ordinary jellium in equilibrium). Thus we make a first-principles prediction of the constant term in the leptodermous expansion of the energy.

Two examples (Al and Na) of the Padé approximation for ordinary jellium are displayed in Fig. 1, together with self-consistent local-density results recalculated with the Perdew-Wang[59] electron-gas input. (In earlier work, Manninen and Nieminen[2] used the Gunnarsson-Lundqvist[72] input.) At the density of Na, no difference can be discerned. At the density of Al, the curves are qualitatively similar but the minimum occurs at −16.3 meV/bohr^2 in the Padé and at −17.5 meV/bohr^2 in the self-consistent result.

Two examples (Al and Na) of the Padé approximation for stabilized jellium are displayed in Fig. 2, together with the self-consistent LDA results of Ref. 28. The good agreement indicates the quality of the Padé representation (30). We believe that these curves should also describe nearly spherical voids in the simple or sp-bonded metals. That the curves of Fig. 2 deviate only slightly from straight lines confirms that (for the simple metals) the domain of validity of the liquid drop model [with only the first two terms of Eqs. (2) or (36)] extends down almost to the atomic scale of sizes, as proposed in Refs. 61 and 62.

From Table II, it can be seen that the values for the curvature energy γ obtained from planar-surface calculations with the fourth order gradient expansion for the kinetic energy[44] and from self-consistent void calculations[28] differ only slightly. If one uses in Eq. (33) the latter value for Al, then σ_R^v changes for $R=2$ bohr from 0.457 to 0.467 millihartree/bohr^2. And the Padé results for the monovacancies hardly change under such substitutions, as shown in Table II.

In Table IV, we compare the Padé representation of Eq. (30) against the results of the self-consistent calculations for monovacancies. Again, the agreement is rather close. Moreover, the monovacancy formation energies predicted for stabilized jellium are in rough agreement with measured values[2–5,7] for the simple metals; for the alkalis, the agreement is excellent. [A recent detailed

TABLE III. Padé parameters of Eqs. (30)–(35) for stabilized jellium and (in parentheses) for ordinary jellium.

Metal	(r_s,z)	A_1	A_2	B_1	B_2	B_3
Al	(2.07, 3)	0	0	0.743	0.325	0.123
		(1.352)	(−0.015)	(0.218)	(0.310)	(−0.004)
Mg	(2.65, 2)	0	0	0.553	0.328	0.139
		(−1.476)	(−0.451)	(0.348)	(0.344)	(0.105)
Na	(3.93, 1)	0	0	0.400	0.286	0.146
		(−0.042)	(−0.021)	(0.389)	(0.289)	(0.146)
Cs	(5.62, 1)	0	0	0.316	0.224	0.144
		(0.098)	(0.064)	(0.453)	(0.700)	(0.130)

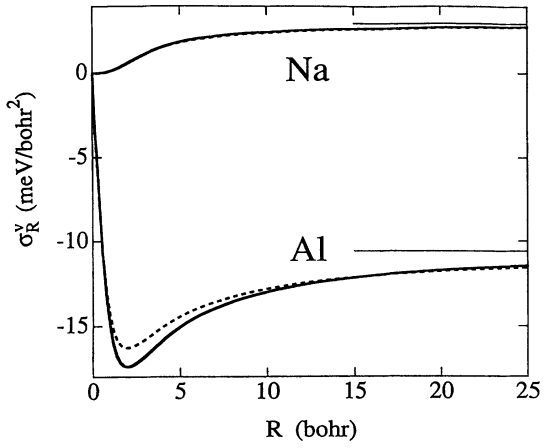

FIG. 1. Void surface energy σ_R^v (meV/bohr^2) of ordinary jellium vs the void radius R (bohr) in the Padé representation (dashed line) of Eq. (30), compared to the results of self-consistent calculations (solid line).

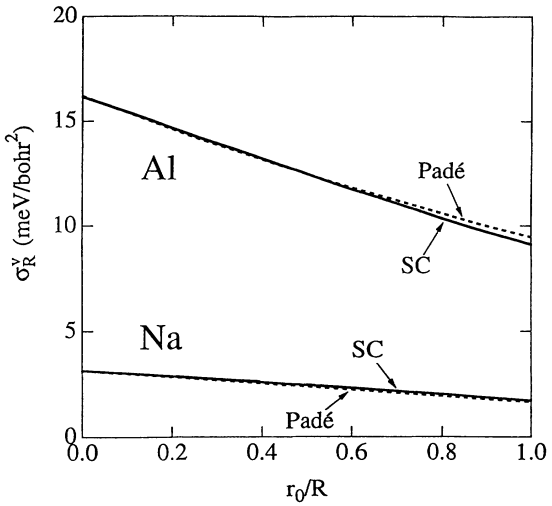

FIG. 2. Void surface energy σ_R^v (meV/bohr^2) of stabilized jellium vs the inverse of the void radius R (in units of $r_0=z^{1/3}r_s$) in the Padé representation of Eq. (30) (dashed line), compared to the results of self-consistent (SC) calculations (Ref. 28) (full line) for Al ($z=3$, $r_s=2.07$) and for Na ($z=1$, $r_s=3.93$). (For plots of σ_R^v vs R, see Ref. 30.)

LDA calculation[18] for Al yields vacancy formation energies 0.83 and 0.73±0.10 eV, respectively without and with lattice relaxation. And recent measurements[5] yield a value of 0.73±0.04 eV for the void formation enthalpy (at 500–650 K), differing slightly from the usually accepted value 0.68±0.03 eV. For Li, an *ab initio* pseudopotential study,[73] including structural relaxation, yields a monovacancy formation energy of 0.54 eV; for Na, the value is 0.34 eV.]

Table V shows the term-by-term convergence of the extended liquid drop expansion of Eq. (36) for the monovacancy formation energies, again at the densities of Al, Mg, Na, and Cs. This table also shows how accurately the Padé approximation predicts the monovacancy formation energies found in self-consistent calculations.[28]

With a negative value of R, Eqs. (2), (36), and (30) describe the nonoscillatory part[28,38] of the surface contribution to the energy of nearly spherical clusters (solid spheres) of a simple metal. For the Wigner-Seitz radius $R=r_0$ (describing a "cluster" consisting of only one atom), the quantity $4\pi r_0^2\sigma^v_{-r_0}$ estimates the cohesive energy.[61] Table VI shows the term-by-term convergence of an extended liquid drop expansion like Eq. (36) for the cohesive energies at the same densities as in Tables III and V.

TABLE IV. Monovacancy formation energies $4\pi r_0^2\sigma^v_{r_0}$ of stabilized jellium in the Padé representation of Eq. (30), compared to the results of self-consistent (SC) calculations (Ref. 28) and to experimental values for real metals. $r_0=z^{1/3}r_s$. (Energy is in electron volts.)

		Padé		SC	
Metal	(r_s,z)	J	SJ	SJ	expt.
H	(1.58, 1)	−2.35	0.24		
Al	(2.07, 3)	−1.77	1.06	1.02	0.73±0.04[a]
Zn	(2.30, 2)	−0.72	0.77	0.74	0.54±0.03[b]
Pb	(2.30, 4)	−1.03	1.39	1.37	0.58±0.04[b]
Mg	(2.65, 2)	−0.12	0.76	0.75	0.58,0.81[b]
Li	(3.24, 1)	0.16	0.37	0.37	0.48[c,b]
Ca	(3.27, 2)	0.37	0.69	0.70	
Sr	(3.57, 2)	0.48	0.66	0.67	
Ba	(3.71, 2)	0.52	0.64	0.65	
Na	(3.93, 1)	0.30	0.33	0.34	0.335[b]
K	(4.86, 1)	0.34	0.28	0.29	0.34[b]
Rb	(5.20, 1)	0.34	0.27	0.27	0.27[d]
Cs	(5.62, 1)	0.32	0.24	0.26	0.28[e]

[a]Reference 5.
[b]Reference 3.
[c]Reference 7.
[d]Reference 2.
[e]Reference 4.

TABLE V. Monovacancy formation energies of stabilized jellium in the extended liquid drop expansion of Eq. (36) and in the Padé representation of Eq. (30). The values in parentheses result from self-consistent void calculations (Ref. 28). Here $R=r_0$ is the void radius. (All energies are in electron volts.)

Metal	$\sigma\cdot 4\pi R^2$	$\sigma\cdot 4\pi R^2-\gamma\cdot 2\pi R$	$\sigma\cdot 4\pi R^2-\gamma\cdot 2\pi R+\delta$	$\sigma_R^v\cdot 4\pi R^2$
Al	1.81	0.88	1.08	1.06 (1.02)
Mg	1.30	0.73	0.71	0.76 (0.75)
Na	0.61	0.36	0.29	0.33 (0.34)
Cs	0.41	0.28	0.23	0.24 (0.26)

Only for metallic hydrogen (not shown in Tables V and VI) do we find poor convergence of the liquid drop expansions for the monovacancy formation and cohesive energies.

V. GENERALIZED LIQUID DROP MODEL FOR CURVED SIMPLE-METAL SURFACES. APPLICATION TO EDGES AND STEPS

In Ref. 30, a generalized liquid drop model was suggested for the energy of a stable simple-metal surface curved on the atomic scale. The expression[74]

$$\sigma\int dA\left[\frac{1}{1-C_1\mathcal{R}^{-1}+C_2\mathcal{R}^{-2}-C_3\mathcal{R}^{-3}}-1\right], \quad (38)$$

where $\mathcal{R}^{-1}$ is the local curvature and $C_n=B_n r_s^n$, should describe the additional total energy arising from the curvature. Planar surface elements with $\mathcal{R}^{-1}=0$ do not contribute. The coefficients C_1, C_2, and C_3 can be obtained from Eqs. (31)–(33), or alternatively from self-consistent calculations for voids in stabilized jellium.[28]

In the following, we use this idea to estimate the edge formation energy of a simple metal, omitting all atomistic detail. Imagine two plane faces of stabilized jellium meeting at an angle θ, the edge they form being rounded with principal curvature radii $r(\gtrsim r_0)$ and ∞, i.e., with curvature $\frac{1}{2}r^{-1}$ for $\theta<\pi$ and $-\frac{1}{2}r^{-1}$ for $\theta>\pi$. From (38), we find that the energy per unit length needed to bend the edge is $(\pi-\theta)r\sigma f(2r)$, where

$$f(x)=\frac{1}{1-C_1/x+C_2/x^2-C_3/x^3}-1\ . \quad (39)$$

So we have, for a 90° edge, $(\pi/2)r\sigma f(2r)$, and, for a 270° edge, $(\pi/2)r\sigma f(-2r)$. The sum of these edge formation energies,

$$\frac{\pi}{2}r\sigma[f(2r)+f(-2r)]\ ,$$

is the additional energy (per unit length) to cleave a bulk of stabilized jellium into a 90° wedge or quarter space and its 270° complementary counterpart or three-quarter space. "Additional" means the following: arising from the curvature at the rounded edges, in addition to the usual cleavage energy of $2\sigma\int dA$. For $r\to\infty$, this additional energy vanishes naturally. For atomically rounded edges of Al ($r=r_0=2.99$) we find, for stabilized jellium and using Tables II and III, 0.81 and -0.65 millihartree/bohr for the 90° and 270° edges, respectively. The sum gives 0.16 millihartree/bohr.

Application of Eq. (38) to a monatomic step of height h with maximally rounded edges of a planar surface of stabilized jellium yields for the step-formation energy per unit length

$$\left[\frac{\pi}{2}-1\right]h\sigma+\frac{\pi}{2}\frac{h}{2}\sigma[f(h)+f(-h)]\ . \quad (40)$$

For a monatomic step on an Al(111) surface, with a step height $h=a/\sqrt{3}$ and a lattice constant $a=7.52$ bohr ($r_s=2.04$, $r_0=2.94$), the two terms of Eq. (40) yield 1.5 and 0.2 millihartree/bohr, using $\sigma=0.61$ and $\gamma/2r_s=0.47$ (both in millihartree/bohr^2), $br_s^3=5.10$ bohr^3, and $cr_s^4=-13.67$ bohr^4 extrapolated from Tables I and II. A detailed calculation by Scheffler, Neugebauer, and Stumpf[31] shows a step-formation energy of 1.7 millihartree/bohr, close to the value 1.8 millihartree/bohr from Eq. (40).

A cruder version[30] of these estimates, based upon Eq. (2) instead of Eq. (38), follows from $f(x)\approx\gamma/(2\sigma x)$.

ACKNOWLEDGMENTS

The work of one of the authors (J.P.) was supported by the U.S. National Science Foundation under Grant No. DMR92-13755. That of two of the authors (J.P. and C.F.) was supported by NATO Collaborative Research

TABLE VI. Cohesive energies of stabilized jellium in an extended liquid drop expansion like Eq. (36) and in the Padé representation of Eq. (30). The values in parentheses result from self-consistent cluster calculations within the spin-unpolarized LDA (Ref. 28) and the local spin density approximation (Ref. 38). Here $R=r_0$ is the cluster (sphere) radius. (All energies are in electron volts.)

Metal	$\sigma\cdot 4\pi R^2$	$\sigma\cdot 4\pi R^2+\gamma\cdot 2\pi R$	$\sigma\cdot 4\pi R^2+\gamma\cdot 2\pi R+\delta$	$\sigma_{-R}^v 4\pi R^2$
Al	1.81	2.75	2.95	3.02 (3.96, 3.79)
Mg	1.30	1.88	1.86	1.87 (1.16, 1.16)
Na	0.61	0.85	0.77	0.82 (1.19, 0.92)
Cs	0.41	0.54	0.49	0.54 (0.74, 0.56)

Grant No. 910623. Another author (P.Z.) acknowledges the hospitality of Tulane University, that of Professor P. H. Dederichs and the Institut für Festkörperforschung of the Forschungszentrum Jülich, that of Professor R. Car and the Institut Romand de Recherche Numerique en Physique des Materiaux Lausanne, that of Professor Yu Lu and the International Centre for Theoretical Physics Trieste, and that of Professor R. M. Nieminen and the Laboratory of Physics of the Helsinki University of Technology, he also appreciates computational help by R. Zeller and M. J. Puska, and helpful remarks by V. Heine, A. Holas, and P. Hautojärvi. We are grateful to M. Scheffler, M. Fähnle, and K. Mosig for providing us with unpublished results.

APPENDIX A: PROOF OF THE VOID THEOREM (8)

To derive the void theorem (8), we need to apply

$$3\bar{n}\frac{d}{d\bar{n}}=3\bar{n}\frac{\partial}{\partial\bar{n}}-R_1\frac{\partial}{\partial R_1} \tag{A1}$$

to E and E_R, the ground-state energies of $\hat{H}$ and $\hat{H}+\hat{H}^{v}_{R}$. The combination in Eq. (A1) ensures neutrality, because $N_1=(4\pi/3)R_1^3\bar{n}$. With

$$3\bar{n}\frac{d}{d\bar{n}}n_+(r)=3\bar{n}\left[\theta(R_1-r)-\frac{R_1}{3}\delta(R_1-r)\right], \tag{A2}$$

and (following from this)

$$3\bar{n}\frac{d}{d\bar{n}}\mathcal{E}_+(r)=4\pi\bar{n}\theta(R_1-r)r, \tag{A3}$$

the Hellmann-Feynman theorem applied to Eq. (5) yields

$$3\bar{n}\frac{dE}{d\bar{n}}=\int d^3r\,\mathcal{E}(r)\bar{n}\theta(R_1-r)r-3\bar{n}\frac{d\bar{e}}{d\bar{n}}N_1 -3\left[\left[\bar{n}\frac{d}{d\bar{n}}\right]^2 e\right](N_1-N_{R_1})+3\frac{de}{d\bar{n}}n(R_1)N_1, \tag{A4}$$

where $n(r)$and $\mathcal{E}(r)$ are the electron density and the electric field of the reference sphere (R_1), respectively, and N_{R_1} is the number of electrons that have spilled out into the vacuum region $r>R_1$.

With

$$3\bar{n}\frac{d}{d\bar{n}}[n_+(r)+n^{v}_{+}(r)] =3\bar{n}\left[\theta(r-R)\theta(R_2-r)-\frac{R_1^3}{3R_2^2}\delta(R_2-r)\right], \tag{A5}$$

and (following from this)

$$3\bar{n}\frac{d}{d\bar{n}}[\mathcal{E}_+(r)+\mathcal{E}^{v}_{+}(r)] =4\pi\bar{n}\theta(r-R)\theta(R_2-r)\frac{r^3-R^3}{r^2}, \tag{A6}$$

application of the Hellmann-Feynman theorem to Eqs. (5) and (6) yields

$$3\bar{n}\frac{dE_R}{d\bar{n}}=\int d^3r\,\mathcal{E}_R(r)\bar{n}\theta(r-R)\theta(R_2-r)\frac{r^3-R^3}{r^2}-3\bar{n}\frac{d\bar{e}}{d\bar{n}}N_2-3\left[\left[\bar{n}\frac{d}{d\bar{n}}\right]^2 e\right](N_2-N_{R_2}-N_R)+3\frac{de}{d\bar{n}}n_R(R_2)N_1 . \tag{A7}$$

$\mathcal{E}_R(r)$ is the electric field of the enlarged sphere (R_2) with the void at its center. Note

$$N_2=\frac{4\pi}{3}(R_2^3-R^3)\bar{n}=\frac{4\pi}{3}R_1^3\bar{n}=N_1 .$$

N_{R_2} and N_R are the number of electrons that have spilled out into the regions $r>R_2$ and $r<R$, respectively.

The difference of (A7) and (A4) can be written as

$$3\bar{n}\frac{d}{d\bar{n}}(E_R-E)=4\pi\bar{n}\int_R^{R_3}dr(r^3-R^3)\mathcal{E}_R(r)+3\left[\left[\bar{n}\frac{d}{d\bar{n}}\right]^2 e\right]N_R+4\pi\bar{n}\left[\int_{R_3}^{R_2}dr(r^3-R^3)\mathcal{E}_R(r)-\int_0^{R_1}dr\,r^3\mathcal{E}(r)\right] +3\left[\left[\bar{n}\frac{d}{d\bar{n}}\right]^2 e\right](N_{R_2}-N_{R_1})+3\frac{de}{d\bar{n}}[n_R(R_2)-n_R(R_1)]N_1 , \tag{A8}$$

where R_3 is in the "bulk" between R and R_1 and increases with increasing R_1. In the limit $R_1\to\infty$,

$$n_R(R_2),n(R_1)\to n(s=0) ,$$

$$N_{R_2}\to 4\pi(R_1^2+2R_1\Delta R_1)\nu, \quad N_{R_1}\to 4\pi R_1^2\nu ,$$

$$\int_{R_3}^{R_2}dr(r^3-R^3)\mathcal{E}_R(r)\to(R_2^3-R^3)\int_{-\infty}^{0}ds\,\mathcal{E}(s) ,$$

$$\int_0^{R_1}dr\,r^3\mathcal{E}(r)\to R_1^3\int_{-\infty}^{0}ds\,\mathcal{E}(s) .$$

Here $n(s)$, ν, and $\mathcal{E}(s)$ refer to the half-space stabilized jellium, and

$$\Delta R_1 \approx \frac{1}{3}\frac{R^3}{R_1^2} \to 0 .$$

With relations of the type of Eq. (14), the last three terms of Eq. (A8) vanish, and Eq. (8) is found after dividing by the void surface area $4\pi R^2$.

From Eq. (A4), the sphere theorem (11) is also easily obtained.

APPENDIX B: PARTIALLY EMPTIED VOID

With

$$n_+^x(r) = -x\bar{n}\theta(R-r) + \bar{n}\theta(r-R_1)\theta(R_x-r) \tag{B1}$$

instead of Eq. (3), and $R_x^3 = R_1^3 + xR^3$, we consider an intermediate step when forming the void by gradually emptying the region $0<r<R$: $x=0$ means no void, $x=1$ means full void, and intermediate situations with $0<x<1$ we refer to as inclusions with lower density. In this case,

$$\frac{\partial \sigma_R^x}{\partial x} = -\frac{R}{3}\bar{n}^2\frac{de}{d\bar{n}} - \frac{R}{3}\bar{n}\left[\int_0^R dr \left[\frac{r}{R}\right]^3 \mathcal{E}_R^x(r) + \int_R^\infty dr\, \mathcal{E}_R^x(r)\right] + \bar{n}\frac{de}{d\bar{n}}\nu_R^x . \tag{B2}$$

$\mathcal{E}_R^x(r)$ is the electric field and ν_R^x is the number of electrons in the partially emptied region $0<r<R$ per unit area.

Small-R expansion of the rhs leads automatically to an explicit dependence on x. Coupling-constant integration of Eq. (B2) therefore yields the small-R expansion

$$\sigma_R^x = x^2\frac{4}{9}\bar{n}^2\int_0^\infty dq[\tilde{\theta}(qR)]^2\left\{1+\left[\frac{4\pi}{q^2}+2\frac{de}{d\bar{n}}+\left[\frac{de}{d\bar{n}}\right]^2\frac{q^2}{4\pi}\right]\frac{\chi(q)}{\tilde{\epsilon}(q)}\right\}R^4+\cdots . \tag{B3}$$

For $x=1$, the result (B3) agrees with Eqs. (19) and (26).

APPENDIX C: PARTIALLY STABILIZED VOID

Here we consider the stabilization corrections to be switched on between $\lambda=0$ (ordinary jellium) and $\lambda=1$ (full stabilized jellium). In this case,

$$\frac{\partial \sigma_R^v(\lambda)}{\partial\lambda} = \bar{n}\frac{de}{d\bar{n}}\nu_R^v(\lambda) . \tag{C1}$$

Small-R expansion of $\nu_R^v(\lambda)$ makes the λ-dependence explicit, and coupling-constant integration of Eq. (C1) yields

$$\sigma_R^v(\lambda) = \sigma_R^v(0) + \lambda\frac{\bar{n}^2}{3}\frac{de}{d\bar{n}}\left[R+\frac{8}{3}\int_0^\infty dq[\tilde{\theta}(qR)]^2\frac{\chi(q)}{\tilde{\epsilon}(q)}R^4\right] + \lambda^2\frac{4}{9}\left[\bar{n}\frac{de}{d\bar{n}}\right]^2\int_0^\infty dq[\tilde{\theta}(qR)]^2\frac{q^2\chi(q)}{4\pi\tilde{\epsilon}(q)}R^4+\cdots , \tag{C2}$$

where

$$\sigma_R^v(0) = -\frac{\bar{n}^2}{3}\frac{de}{d\bar{n}}R + \frac{4\pi}{15}\bar{n}R^3 + \frac{4}{9}\bar{n}^2\int_0^\infty dq[\tilde{\theta}(qR)]^2\frac{4\pi\chi(q)}{q^2\tilde{\epsilon}(q)}R^4+\cdots . \tag{C3}$$

For $\lambda=1$ (full stabilization), $\sigma_R^v(1)=\sigma_R^v$ emerges.

APPENDIX D: PHYSICAL DERIVATION OF THE SMALL-R EXPANSION FOR THE ENERGY OF A VOID IN ORDINARY JELLIUM

We imagine forming the spherical void by the following steps: (a) Change the electron number in the system by $\delta N_e = -\bar{n}4\pi R^3/3$. The energy cost is $\mu\delta N_e$, where μ is the chemical potential. (b) Prepare a sphere of "negative background" with density $-\bar{n}$, radius R, and charge δN_e. The energy cost is the electrostatic self-energy $(3/5)(\delta N_e)^2/R$. (c) Plunge this sphere of "negative background" into the jellium. The first-order energy change is $-\bar{\phi}\delta N_e$, where $\bar{\phi}$ is the average electrostatic potential energy of an electron inside the jellium. The second-order change is given by Eq. (22) with $de/d\bar{n}$ replaced by zero.

The total energy cost of steps (a), (b), and (c) is thus

$$-e\bar{n}\frac{4\pi}{3}R^3 + \sigma_R^v 4\pi R^2 = (\bar{\phi}-\mu)\bar{n}\frac{4\pi}{3}R^3 + \frac{3}{5}\left[\frac{4\pi}{3}\right]^2\bar{n}^2R^5+\beta R^6+\cdots . \tag{D1}$$

From this equation, we find σ_R^v in the form of Eq. (1). The coefficient a of the leading term is simplified by the relationship[34]

$$\mu = \bar{\phi} + \frac{d}{d\bar{n}}(\bar{n}e) . \tag{D2}$$

*Permanent address: Many-Body Problems Group, P.O. Box 410113, D-01224 Dresden, Germany.

[1]Measured vacancy formation energies of several metals are found in Refs. 2–4. For recent measurements of the vacancy formation entropy and enthalpy of Al, see Ref. 5. For a general relation between formation energy (at constant volume) and formation enthalpy (at constant pressure), see Ref. 6. For the recently measured vacancy formation energy of Li, see Ref. 7. References for vacancy formation energies of fcc transition metals can be found in Ref. 8.

[2]M. Manninen and R. M. Nieminen, J. Phys. F **8**, 2243 (1978), and references therein.

[3]*Numerical Data and Functional Relationships in Science and Technology III,* edited by H. Ullmaier, Landolt-Börnstein, New Series, Group III, Vol. 25 (Springer-Verlag, Berlin, 1991).

[4]Ya. A. Kraftmakher and P. G. Strelkov, in *Vacancies and Interstitials in Metals,* edited by A. Seeger, D. Schumacher, W. Schilling, and J. Diehl (North-Holland, Amsterdam, 1970), p. 59.

[5]K. Mosig (private communication); and K. Mosig, J. Wolff, J.-E. Kluin, and Th. Hehenkamp, J. Phys. Condens. Matter **4**, 1447 (1992).

[6]G. Jacucci and R. Taylor, J. Phys. F **9**, 1489 (1979).

[7]H. Schultz, Mater. Sci. Eng. A **141**, 149 (1991).

[8]B. Drittler, M. Weinert, R. Zeller, and P. H. Dederichs, Solid State Commun. **79**, 31 (1991).

[9]M. Eldrup, in *Positron Annihilation,* edited by Zs. Kajcsos and Cs. Szeles (Trans Tech Publications, Aedermannsdorf/Switzerland, 1992), p. 229; see also Refs. 10–12.

[10]M. Manninen, R. Nieminen, P. Hautojärvi, and J. Arponen, Phys. Rev. B **12**, 4012 (1975).

[11]P. Jena, A. K. Gupta, and K. S. Singwi, Solid State Commun. **21**, 293 (1977).

[12]P. Hautojärvi, J. Heiniö, M. Manninen, and R. Nieminen, Philos. Mag. **35**, 973 (1977).

[13]R. Nieminen, M. Manninen, P. Hautojärvi, and J. Arponen, Solid State Commun. **16**, 831 (1975).

[14]R. Evans and M. W. Finnis, J. Phys. F **6**, 483 (1976).

[15]M. W. Finnis and R. M. Nieminen, J. Phys. F **7**, 1999 (1977).

[16]I. Gyémant and G. Solt, Phys. Status Solidi B **82**, 651 (1977).

[17]R. M. Nieminen, J. Nucl. Mater. **69**, 633 (1978).

[18]P. J. H. Denteneer and J. M. Soler, J. Phys. Condens. Matter **3**, 8777 (1991).

[19]M. J. Mehl and B. M. Klein, Physica B **172** (1&2), 211 (1991).

[20]J. Furthmüller and M. Finnis (private communication); Europhys. Conf. Abstr. **17A**, 1257 (1993).

[21]A. Seeger and M. Fähnle, in *Computer Aided Innovation of New Materials II,* edited by M. Doyama, J. Kihara, M. Tanaka, and R. Yamamoto (Elsevier, Amsterdam, 1993), p. 439.

[22]R. Zeller, B. Drittler, P. Lang, K. Abraham, and P. H. Dederichs, *Electronic Structure of Solids '91,* edited by P. Ziesche and H. Eschrig (Akademie Verlag, Berlin, 1991), p. 57.

[23]P. H. Dederichs, T. Hoshino, B. Drittler, K. Abraham, and R. Zeller, Physica B **172** (1&2), 203 (1991).

[24]For this method with its applications to the electronic properties of point defects in metals, see I. Mertig, E. Mrosan, and P. Ziesche, *Multiple Scattering Theory of Point Defects in Metals: Electronic Properties* (Teubner, Leipzig, 1987).

[25]K. Willenborg, Diplomarbeit TH Aachen/IFF Jülich, 1992.

[26]M. Brack, Rev. Mod. Phys. **65**, 677 (1993).

[27]C. A. Utreras-Díaz and H. B. Shore, Phys. Rev. Lett. **53**, 2335 (1984).

[28]P. Ziesche, M. J. Puska, T. Korhonen, and R. M. Nieminen, J. Phys. Condens. Matter **5**, 9049 (1993).

[29]G. Schreckenbach, R. Kaschner, and P. Ziesche, Phys. Rev. B **46**, 7864 (1992).

[30]J. P. Perdew, P. Ziesche, and C. Fiolhais, Phys. Rev. B **47**, 16 460 (1993).

[31]M. Scheffler, J. Neugebauer, and R. Stumpf, J. Phys. Condens. Matter **5**, A91 (1993).

[32]H. Ishida and A. Liebsch, Phys. Rev. B **46**, 7153 (1992).

[33]N. D. Lang and W. Kohn, Phys. Rev. B **1**, 4555 (1970). A recent treatment of planar jellium surfaces with the help of correlated many-body wave functions is reported by X.-P. Li, R. J. Needs, R. M. Martin, and D. M. Ceperley, *ibid.* **45**, 6125 (1992).

[34]N. D. Lang and W. Kohn, Phys. Rev. B **3**, 1215 (1971).

[35]N. W. Ashcroft and D. C. Langreth, Phys. Rev. **155**, 682 (1967).

[36]R. Monnier and J. P. Perdew, Phys. Rev. B **17**, 2595 (1978); **22**, 1124(E) (1980).

[37]J. P. Perdew, H. Q. Tran, and E. D. Smith, Phys. Rev. B **42**, 11 627 (1990). See also Ref. 38.

[38]M. Brajczewska, C. Fiolhais, and J. P. Perdew, Int. J. Quantum Chem. Symp. **27**, 249 (1993). See also J. P. Perdew, M. Brajczewska, and C. Fiolhais, Solid State Commun. **88**, 795 (1993).

[39]H. B. Shore and J. H. Rose, Phys. Rev. Lett. **66**, 2519 (1991). The "ideal metal" proposed in this reference has the same surface properties as the "stabilized jellium" of Ref. 37, but less-satisfactory bulk properties, as shown by J. M. Soler, *ibid.* **67**, 3044 (1991).

[40]E. G. Brovman and Yu. M. Kagan, in *Dynamical Properties of Solids, Vol. 1: Crystalline Solids, Fundamentals,* edited by G. K. Horton and A. A. Maradudin (North-Holland, Amsterdam, 1974), p. 191, and references therein.

[41]A. Holas, in Proceedings of the Mini-Workshop on Quantum and Classical Many-Body Theory in Condensed Matter Physics, ICTP Trieste, July 22–Aug. 2, 1991 (in press).

[42]V. Heine and C. H. Hodges, J. Phys. C **5**, 225 (1972), and references therein.

[43]J. H. Rose and H. B. Shore, Phys. Rev. B **43**, 11 605 (1991).

[44]C. Fiolhais and J. P. Perdew, Phys. Rev. B **45**, 6207 (1992).

[45]A. Kiejna, Phys. Rev. B **47**, 7361 (1993).

[46]A. Kiejna, P. Ziesche, and R. Kaschner, Phys. Rev. B **48**, 4811 (1993); A. Kiejna and P. Ziesche, Solid State Commun. **88**, 143 (1993).

[47]M. Mansfield and R. J. Needs, Phys. Rev. B **43**, 8829 (1991).

[48]T. L. Ainsworth and E. Krotscheck, Phys. Rev. B **45**, 8779 (1992).

[49]B. Montag, Diplomarbeit, Universität Erlangen, 1993.

[50]B. Montag, P.-G. Reinhard, E. Chabanat, J. Meyer, and M. Seidl, Europhys. Conf. Abstr. **17A**, 1643 (1993).

[51]Ll. Serra, G. B. Bachelet, Nguyen Van Giai, and E. Lipparini, Phys. Rev. B **48**, 14 708 (1993).

[52]D. Lehmann and P. Ziesche, Solid State Commun. **56**, 847 (1985).

[53]W. Ekardt, J. Kühn, D. Lehmann, and P. Ziesche, Solid State Commun. **64**, 1371 (1987).

[54]D. Lehmann and P. Ziesche, Helv. Physica Acta **57**, 621 (1984).

[55]H. F. Budd and J. Vannimenus, Phys. Rev. Lett. **31**, 1218 (1973); **31**, 1430(E) (1973). Their relation (3) agrees with Eq. (2.43) of A. Theophilou, J. Phys. F **2**, 1124 (1974) for $F=0$. From the interpretation of the Theophilou or Budd-Vannimenus theorem [with $E(s)$ on its rhs] as a force sum rule, its generalization for crystals was derived in Refs. 56

and 57. This generalization provides a qualitative understanding of alternating multilayer relaxations at planar surfaces of half-space-filling crystals.

[56]R. Kaschner and P. Ziesche, Phys. Scr. **38**, 414 (1988).

[57]P. Ziesche and R. Kaschner, Phys. Status Solidi B **145**, K9 (1988).

[58]J. Vannimenus and H. F. Budd, Solid State Commun. **15**, 1739 (1974).

[59]J. P. Perdew and Y. Wang, Phys. Rev. B **45**, 13 244 (1992).

[60]J. P. Perdew and T. Datta, Phys. Status Solidi B **102**, 283 (1980).

[61]J. P. Perdew, Y. Wang, and E. Engel, Phys. Rev. Lett. **66**, 508 (1991).

[62]E. Engel and J. P. Perdew, Phys. Rev. B **43**, 1331 (1991).

[63]G. Makov and A. Nitzan, Phys. Rev. B **47**, 2301 (1993).

[64]This procedure is similar to that of Budd and Vannimenus (Ref. 55), who derived the linear force constant for the cohesive force by inserting a thin negatively charged slab into an otherwise homogeneous jellium, thus creating a small separation between two half-space jellia.

[65]P. Ziesche and D. Lehmann, J. Phys. C **16**, 879 (1983).

[66]P. Ziesche and R. Kaschner, Solid State Commun. **78**, 703 (1991).

[67]R. Kaschner, Ph.D. thesis, Technische Universität Dresden, 1989.

[68]V. V. Pogosov, Solid State Commun. **75**, 469 (1990).

[69]While $\epsilon=1-4\pi\tilde{\chi}/q^2$ with $\tilde{\chi}=\chi/[1+G4\pi\chi/q^2]$ describes the linear screening of an external perturbation due to a weak test charge, $\tilde{\epsilon}=1-(1-G)4\pi\chi/q^2$ describes the screening of an electron that belongs to the system and thus polarizes its surroundings (local field); cf., e.g., G. Lehmann and P. Ziesche, *Electronic Properties of Metals* (Elsevier, Amsterdam, 1990), p. 125.

[70]W. Kohn and L. J. Sham, Phys. Rev. **140**, A1133 (1965).

[71]K. Willenborg, R. Zeller, P. H. Dederichs, and P. Ziesche (unpublished); P. Ziesche, A. Seitsonen, M. Puska, and R. Nieminen (unpublished).

[72]O. Gunnarsson and B. I. Lundqvist, Phys. Rev. B **13**, 4274 (1976).

[73]W. Frank, U. Breier, C. Elsässer, and M. Fähnle, Phys. Rev. B **48**, 7676 (1993); U. Breier, W. Frank, C. Elsässer, and M. Fähnle (unpublished).

[74]The liquid drop model and its generalization (30) seem to work better at smaller ratios $\gamma/2\sigma r_0$. The ratios for Cs, Na, Mg, and Al are 0.32, 0.40, 0.44, and 0.52, respectively.